

# Effect of Mixing Oils on the Hexagonal Liquid Crystalline Structures

Hironobu Kunieda,\* Go Umizu, and Kenji Aramaki

Division of Artificial Environment and Systems, Graduate School of Engineering, Yokohama National University, Tokiwadai 79-5, Hodogaya-ku, Yokohama 240-8501, Japan

Received: August 20, 1999; In Final Form: December 2, 1999

Structural change in hexagonal liquid crystal ( $H_1$ ) in the water/heptaoxyethylene dodecyl ether ( $C_{12}EO_7$ ) system upon addition of mixed oil (*m*-xylene + decane) is investigated by phase study and small-angle X-ray scattering (SAXS). The surfactant layer curvature tends to be less positive or negative upon addition of the mixed oil at a high *m*-xylene/decane ratio, and the  $H_1$ – $L_\alpha$  (lamellar liquid crystal) transition takes place. At a low *m*-xylene/decane ratio, however, the  $H_1$ – $I_1$  transition occurs with increasing mixed oil content, where  $I_1$  is a discontinuous micellar cubic phase. An excess oil phase directly separates from the  $H_1$  phase at a moderate *m*-xylene/decane ratio. The change in the effective cross sectional area per surfactant,  $a_s$ , as a function of oil content was also measured at each mixing fraction of oils by SAXS. *m*-Xylene molecules tend to penetrate the surfactant palisade layer and widen  $a_s$ , whereas decane molecules tend to be solubilized in the deep core of surfactant hydrophobic moieties and the  $a_s$  is not largely expanded. The  $a_s$  does not jump at each transition of  $H_1$ – $I_1$  and  $H_1$ – $L_\alpha$ . Considering the volume of polyoxyethylene chain (EO chain), the repulsion between the EO chains may increase upon addition of decane, whereas it would decrease upon addition of *m*-xylene. To balance the repulsion with the attraction due to the interfacial tension between water and the lipophilic part without the big change in  $a_s$ , the phase transitions take place but the change in the surfactant layer curvature is opposite in both oil systems.

## Introduction

Cloud temperature in an aqueous nonionic surfactant solution is shifted to lower temperatures upon addition of short-chain alkanes or aromatic hydrocarbons, whereas it increases with long-chain hydrocarbons.<sup>1</sup> This phenomenon is highly related to the change in micellar shape upon addition of oil<sup>2</sup> because the micellar shape is changed because of the difference in the manner of solubilization of oil in the surfactant aggregates.<sup>3</sup> It is also known that the shapes of self-organized structures are highly dependent on the types of oils in water/block copolymer/oil systems.<sup>4</sup>

Oil molecules are solubilized in lipophilic moieties of surfactant aggregates. Short-chain alkanes or aromatic hydrocarbons tend to penetrate the surfactant palisade layers or in the vicinity of the interface of the aggregate.<sup>5–7</sup> On the other hand, long-chain saturated hydrocarbons are solubilized in the deep core of the lipophilic chains. As a result, the curvature of the surfactant layer tends to be negative upon addition of the former oils, where the convex curvature toward water is regarded as positive.<sup>3</sup> The long-chain alkanes, however, have an opposite tendency. Even if oil is fixed, a similar tendency is observed depending on the hydrophilicity of surfactant in the case of polyoxyethylene-type nonionic surfactant.<sup>3</sup> When oil is solubilized in the aggregates in hydrophilic surfactant systems, the surfactant layer curvature remains positive and vice versa. The positive change of the surfactant curvature upon addition of oil would be related to the increase in repulsion of hydrophilic moieties. However, there is no report on the influence of oil solubilization on the repulsion.

In the aqueous nonionic surfactant solutions, the curvature of surfactant self-organized structures such as liquid crystals

successively changes from positive to negative with decreasing polyoxyethylene chain (EO chain) length at constant temperature.<sup>8</sup> Accordingly, the shapes of the liquid crystals are also step by step changed from sphere to reverse sphere via rod, layer, and reverse rod. Since the effect of oil on the surfactant molecular curvature in hydrophilic surfactant systems is opposite that in lipophilic surfactant systems, the surfactant curvature is sharply changed in a very narrow range of the EO chain length of the surfactant in the presence of a sufficient amount of oil. This is the reason the HLB temperature or three-phase temperature<sup>9,10</sup> appears in water/nonionic surfactant/oil systems.

Accordingly, it is very important to understand the structural change of liquid crystals with the addition of oil. In our previous study,<sup>8</sup> the EO chain length of surfactant is changed by using different surfactants or by mixing the surfactants while oil is fixed. However, instead of using a combination of plural surfactants, if a mixture of oils is added to a single surfactant system, it is easier to analyze the effect of oil on the change in self-organized structures.

In this context, we investigated the effect of added mixed oil (*m*-xylene + decane) on the phase behavior and the structures of liquid crystals in the water/heptaoxyethylene dodecyl ether ( $C_{12}EO_7$ ) system.

## Experimental Section

**Materials.** Homogeneous heptaoxyethylene dodecyl ether was obtained from Nikko Chemicals, and it is abbreviated as  $C_{12}EO_7$ . *m*-Xylene (98.0%) was obtained from Wako Pure Chemical. *n*-Decane (99.0%) was obtained from Tokyo Kasei Kogyo. These chemicals were used without further purification.

**Small-Angle X-ray Scattering (SAXS).** Interlayer spacing of liquid crystal was measured by SAXS, performed on a small-angle scattering goniometer with an 18 kW Rigaku Denki

\* To whom correspondence should be addressed. Phone and fax: +81-45-339-4190. E-mail: kunieda@ynu.ac.jp.

rotating anode (Rint-2500) at about 25 °C. The samples of liquid crystals were lapped by plastic films for the measurement (Mylar seal method). The types of liquid crystals were identified by the SAXS peak ratios.<sup>3,8</sup>

**Molar Volumes of Each Functional Group in the Surfactant.** The molar volume of surfactant is calculated by the following equation:

$$V_S = \frac{M_S}{\rho_S} \quad (1)$$

where  $M_S$  and  $V_S$  are the molecular weight and the molar volume of surfactant.  $\rho_S$  is the density of surfactant. The arithmetic additivity holds concerning the molar volumes of each functional group in the surfactant.<sup>8,11</sup> Then the molar volume of the surfactant is the sum of molar volumes of each group in the surfactant, and the following relation holds:

$$V_S = V_L + nV_{EO} + V_{OH} \quad (2)$$

where  $V_L$ ,  $V_{EO}$ , and  $V_{OH}$  are the molar volumes of the lipophilic part, the oxyethylene (EO) group, and the hydroxyl group, respectively, and  $n$  is the number of EO units.  $V_{EO}$  is 38.8, and  $V_{OH}$  is 8.8 cm<sup>3</sup> mol<sup>-1</sup> according to the previous data on C<sub>12</sub>-EO<sub>*n*</sub>.<sup>8,12</sup> From these data and eq 2, the  $V_L$  is calculated to be 215 cm<sup>3</sup> mol<sup>-1</sup>. These values were used to analyze the detailed structure of liquid crystals.

## Results

**Phase Behavior as a Function of Temperature.** Since the phase behavior of nonionic surfactant is highly dependent on temperature, we first investigated the effect of added decane, *m*-xylene, and the mixed oil on the phase behavior of aqueous C<sub>12</sub>EO<sub>7</sub> solution as a function of temperature at a high concentration of surfactant. The results are shown in Figure 1. The volume fraction of the lipophilic part of the surfactant in water + surfactant,  $\phi_L$ , is kept constant (=0.2). This composition corresponds to ~46 wt % of the total surfactant in the system.

In the absence of oil (on the left-hand axis), the surfactant forms a hexagonal liquid crystal ( $H_1$ ) at low temperature and the  $H_1$  phase melts to an aqueous micellar solution ( $W_m$ ) with increasing temperature. With a further increase in temperature, the  $W_m$  phase splits into two isotropic phases at the cloud temperature.

In the decane system, the discontinuous micellar cubic phase ( $I_1$ ) appears upon a small addition of oil at a low temperature. This phenomenon is known in other surfactant systems.<sup>13,14</sup> It is considered that spherical or spherical-like micelles are packed in a cubic array in the  $I_1$  phase.<sup>15,16</sup> In an oil-rich region, the  $I_1$  phase coexists with an excess oil phase (O). At the mid-temperature in the phase diagram, the  $H_1$  phase coexists with the excess oil phase. The lamellar liquid crystal ( $L_\alpha$ ) forms at higher temperature than the  $H_1$  phase as is shown in Figure 1a. Just above the  $L_\alpha$  phase, the isotropic fluid phase ( $D_2$ ) is observed. The  $D_2$  phase also appears in binary water/nonionic surfactant systems,<sup>8</sup> and it is often called the  $L_3$  phase. In our notation of phases, we use the subscripts 1 and 2 for the type of liquid crystals. The "1" means the positive curvature of surfactant layer, whereas the negative curvature is indicated by "2". It is known that the curvature in the  $D_2$  phase is slightly negative.<sup>17,18</sup> At temperatures above the  $D_2$  phase, the reverse micellar solution or the w/o type microemulsion ( $O_m$ ) coexists with an excess water phase (W).

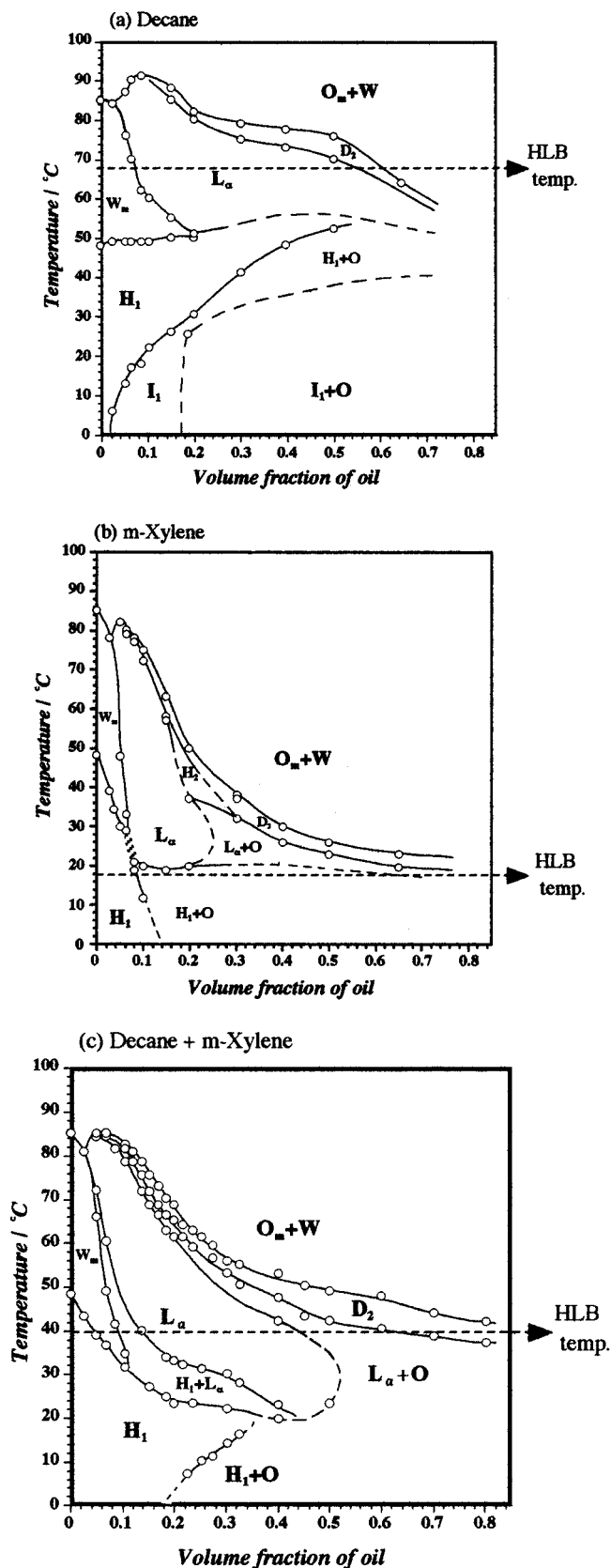


**Figure 1.** Effect of added decane (a), *m*-xylene (b), and the mixed oil (c) on the phase behavior of aqueous C<sub>12</sub>EO<sub>7</sub> solution as a function of temperature. The volume fraction of the lipophilic part of the surfactant in water + surfactant is fixed at 0.2.

It is clear from Figure 1a that the temperature ranges for rod micelles ( $H_1$  phase) and the layer structure ( $L_\alpha$  phase) tend to shrink upon addition of decane and that the spherical micelles

in the  $I_1$  phase changes to the reverse spherical micelles in the  $O_m$  phase in a narrow range of temperature in the presence of oil compared with the oil-free system. In other words, upon addition of decane, the rod–sphere transition of the micellar shape takes place at a low temperature, whereas the layer–reverse sphere transition occurs at a high temperature.

On the other hand, the phase pattern is shifted to lower temperatures and the  $I_1$  phase does not appear in the *m*-xylene system as is shown in Figure 1b. Even at low temperature, the rod–layer ( $H_1$ – $L_\alpha$ ) transition is observed. In the mixed-oil system in Figure 1c, where the decane/*m*-xylene weight ratio is unity, we can see the phase behavior between parts a and b of Figure 1.

The phase behavior is highly related to the HLB temperature at which the microemulsion or surfactant phase coexists with excess water and oil phases in a dilute surfactant system. The surfactant layer is saturated with oil, and its curvature is zero at the HLB temperature. The HLB temperature or the mid-temperature of the three-phase body in a ternary water/nonionic surfactant/oil system can be empirically calculated by<sup>10</sup>

$$T_{\text{HLB}} = k_{\text{oil}}(N_{\text{HLB}} - N_{\text{oil}}) \quad (3)$$

where  $T_{\text{HLB}}$  is the HLB temperature,  $N_{\text{HLB}}$  is Griffin's HLB number,<sup>18</sup> and  $k_{\text{oil}}$  and  $N_{\text{oil}}$  are constant for a particular oil.  $k_{\text{oil}}$  is  $\sim 17$  °C/HLB unit for many oils, and  $N_{\text{oil}}$  is 8.5 for decane and 11.4 for *m*-xylene. Since there is no experimental data for *m*-xylene, we use the value of ethylbenzene for *m*-xylene. The calculated HLB temperatures are  $\sim 68$  °C for decane,  $\sim 19$  °C for *m*-xylene, and  $\sim 40$  °C for the mixed oil, and they are indicated by the broken lines in Figures 1. As is shown in Figure 1, the  $L_\alpha$  phase is extended to an oil-rich region around at the HLB temperature. The surfactant molecular curvature tends to be negative above the HLB temperature, whereas it maintains the positive curvature below the HLB temperature upon addition of oil.

**Phase Behavior at Constant Temperature.** The HLB temperatures are dependent on the type of oil and the mixing ratio of oils. Hence, if we construct a phase diagram of the water/ $C_{12}\text{EO}_7$ /mixed oil system as a function of the mixing fraction of *m*-xylene in the mixed oil at constant temperature, a phase behavior similar to that in Figure 1 should be observed. Figure 2 shows the effect of added mixed oil (*m*-xylene + decane) on the phase behavior of aqueous  $C_{12}\text{EO}_7$  solution as a function of the volume ratio of *m*-xylene to the mixed oil,  $\phi_{\text{xylene}}/\phi_0$ , at 25 °C, where  $\phi_0$  and  $\phi_{\text{xylene}}$  are the volume fractions of *m*-xylene and the mixed oil in the system, respectively. As shown in Figures 1 and 2, the changes in the mixing fraction of oil and temperature are the variables for obtaining similar phase behavior.

At a high decane ratio, the  $H_1$  phase changes to the  $I_1$  phase whereas the  $H_1$  phase changes to the  $D_2$  phase via the  $L_\alpha$  phase at a low decane ratio. In the midst of the phase diagram, the  $H_1$  phase or  $L_\alpha$  phase coexists with excess oil in the oil-rich region. In the center of the phase diagram, the solubilization of oil in the liquid crystals reaches its maximum. Note that reverse vesicles are formed in the  $L_\alpha + O$  region in the oil-rich region because the  $L_\alpha$  phase can swell a large amount of oil. It is clear from Figure 2 that the rod–sphere transition takes place in the decane-rich region whereas the rod–layer transition occurs upon addition of *m*-xylene at constant temperature.

**Structural Change in Liquid Crystals.** We measured the interlayer spacing,  $d$ , of liquid crystals at each mixing ratio of *m*-xylene in the mixed oil. We calculated the effective cross

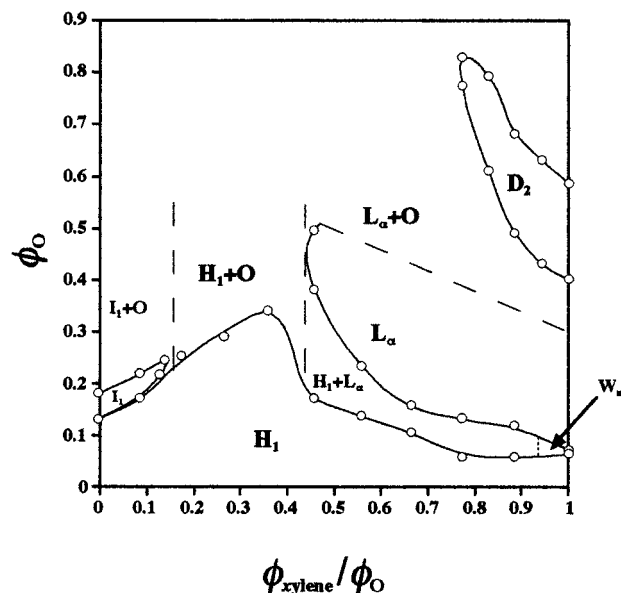


**Figure 2.** Effect of added oil on the phase behavior of aqueous  $C_{12}\text{EO}_7$  solution at 25 °C. The volume fraction of the lipophilic part of the surfactant in water + surfactant is fixed at 0.2.  $\phi_0$  and  $\phi_{\text{xylene}}$  are the volume fractions of the mixed oil and *m*-xylene, respectively.

sectional area per surfactant molecule,  $a_s$ , in the aggregates using the measured  $d$  values. It is assumed that the hexagonal ( $H_1$ ) phase consists of infinitely long cylindrical micelles packed in a hexagonal array and that the lamellar ( $L_\alpha$ ) phase consists of infinitely wide bimolecular layers stacked in a parallel way as is schematically shown in Figure 3. It is also assumed that spherical micelles are packed in a cubic array in the  $I_1$  phase.

According to the geometry of liquid crystals, the  $a_s$  is calculated by the following equations using the  $d$  value obtained from the SAXS measurement. For the  $L_\alpha$  phase,

$$d_{L_\alpha} = \frac{d(\phi_L + \phi_O)}{2} \quad (4)$$

$$a_s = \frac{v_L}{d_{L_\alpha}} \frac{\phi_L + \phi_O}{\phi_L} \quad (5)$$

where  $d_{L_\alpha}$  is half the hydrophobic thickness in the  $L_\alpha$  phase,  $\phi_L$  is the volume fraction of the hydrophobic part of the surfactant in the system, and  $v_L$  is the volume of the hydrophobic part of one surfactant molecule.

For the  $H_1$  phase,

$$r_H = d \sqrt{\frac{2(\phi_L + \phi_O)}{\sqrt{3}\pi}} \quad (6)$$

$$a_s = \frac{2v_L}{r_H} \frac{\phi_L + \phi_O}{\phi_L} \quad (7)$$

where  $r_H$  is the radius of the hydrophobic part of the cylindrical micelle.

For the  $I_1$  phase,

$$r_1 = d \left( \frac{3}{4\pi} \frac{(\phi_L + \phi_O)}{n_c} \right)^{1/3} C \quad (8)$$

$$a_s = \frac{3v_L}{r_1} \frac{\phi_L + \phi_O}{\phi_L} \quad (9)$$

where  $C$  is constant,  $\sqrt{2}$  for body-centered cubic,  $\sqrt{3}$  for face-

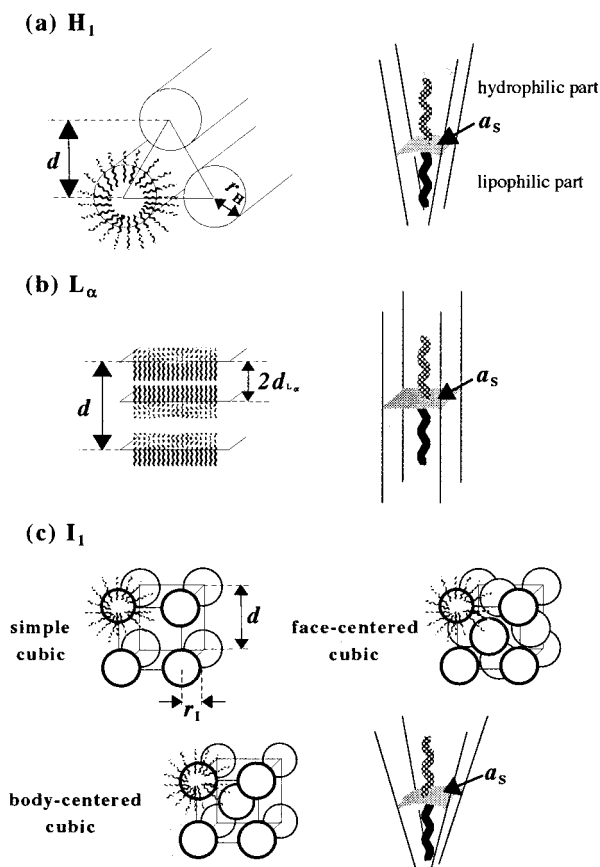


**Figure 3.** Schematic structures of H<sub>1</sub> (a), L<sub>α</sub> (b), and I<sub>1</sub> (c) phases.  $d$  is the interlayer spacing measured by SAXS.  $a_s$  is the effective cross sectional area per surfactant molecule at a hydrophobic interface.

centered cubic, and 1 for simple-cubic structures, respectively.  $n_C$  is the number of micelles in a unit cell, 2 for body-centered cubic, 4 for face-centered cubic, and 1 for simple-cubic structures.  $r_1$  is the radius of the spherical micelle in the I<sub>1</sub> phase. The results are shown in Figure 4.

At a high ratio of decane in the mixed oil,  $a_s$  slightly increases with increasing the oil content, whereas it considerably increases at a high ratio of *m*-xylene in the H<sub>1</sub> phase. Since the decane tends to be solubilized in the deep core of the aggregates compared with *m*-xylene, the  $a_s$  does not increase very much. On the other hand, *m*-xylene tends to be solubilized in the surfactant palisade layer or in the vicinity of the interface, and the  $a_s$  is widened.<sup>3</sup> Since the number of SAXS peaks is not enough to identify the detailed structure of the I<sub>1</sub> phase, we calculated the  $a_s$  for both face- (fcc) and body- (bcc) centered cubic structures. The difference in  $a_s$  for both cubic structures is small as is shown in parts a and b of Figure 4. In the L<sub>α</sub> phase, the  $a_s$  is almost unchanged and only interlayer spacing increases in the *m*-xylene-rich systems. Since the surfactant palisade layer is saturated with oil, the oil core is widened.

As is shown in Figure 4, the radius of the cylinder micelle in the H<sub>1</sub> phase jumps or abruptly changes to that of the spherical micelle in the I<sub>1</sub> phase or the half-thickness of the bilayer in the L<sub>α</sub> phase at each transition point. On the other hand, the  $a_s$  is almost unchanged at the H<sub>1</sub>–I<sub>1</sub> and H<sub>1</sub>–L<sub>α</sub> transitions.

## Discussion

**H<sub>1</sub>–I<sub>1</sub> Transition.** The surfactant layer curvature at the interface of the hydrophobic part of surfactant layers is determined by the balance between the repulsion of hydrophilic moieties and the attraction of lipophilic moieties due to the

interfacial tension of water–lipophilic moieties.<sup>20,21</sup> The repulsion due to hydration, steric hindrance, etc. tends to widen the effective cross sectional area per surfactant,  $a_s$ , whereas the interfacial tension tends to shrink the  $a_s$ .

In the present systems, the hydration of the EO chains can be regarded as being approximately constant, since the water/surfactant ratio is fixed and only the oil content is changed. The H<sub>1</sub> phase changes to the I<sub>1</sub> phase upon addition of oil at a high decane ratio as is shown in Figure 2. The  $a_s$  is slightly increased with increasing oil content in the H<sub>1</sub> phase. The radius of the cylinder jumps to that of the sphere in the I<sub>1</sub> phase at the transition, as shown in Figure 4. Since the  $a_s$  is almost the same value for both H<sub>1</sub> and I<sub>1</sub> phases at each transition point, the radius of the spherical micelle in the I<sub>1</sub> phase is approximately 1.5 times longer than the radius of the cylinder micelle in the H<sub>1</sub> phase.<sup>2</sup> Since decane molecules tend to be solubilized or swollen in the deep core of hydrocarbon chains of the surfactant, the volume of the hydrophobic part of the surfactant palisade layer is not greatly increased.

The surfactant layer curvature at the interface of hydrophobic part of aggregates is calculated by  $1/r_1$  for a spherical micelle and  $1/(2r_H)$  for a cylindrical micelle because the mean curvature ( $1/R_{\text{mean}}$ ) can be expressed by

$$\frac{1}{R_{\text{mean}}} = \frac{1}{2} \left( \frac{1}{R_1} + \frac{1}{R_2} \right) \quad (10)$$

where  $R_{\text{mean}}$  is the radius of the mean curvature and  $R_1$  and  $R_2$  are the radii for two principal curvatures at the interface.  $R_1 = r_H$  and  $R_2 = \infty$  for the H<sub>1</sub> phase, and  $R_1 = R_2 = r_1$  for the I<sub>1</sub> phase. The change in the mean curvature for H<sub>1</sub> and I<sub>1</sub> phases in a decane-rich system is shown in Figure 5. The mean curvature decreases with increasing oil content in the H<sub>1</sub> phase, and it jumps to a high value in the I<sub>1</sub> phase at the transition point. When the surfactant molecules form a spherical micelle, the average effective cross sectional area of the EO chain becomes large even at constant  $a_s$ , compared with that in the H<sub>1</sub> phase, as shown in Figure 3. The greater the distance from the interface, the wider the effective cross sectional or occupied area of the EO chain is. Namely, the repulsion decreases when the rod–sphere transition takes place. Hence, it is considered that the repulsion between the EO chains would be increased when oil is solubilized in the deep core of the cylinder micelle. Finally, the relaxation of the repulsion may occur at the H<sub>1</sub>–I<sub>1</sub> transition.

**H<sub>1</sub>–L<sub>α</sub> Transition.** The surfactant curvature tends to be 0 or negative upon addition of *m*-xylene or the mixed oil of high *m*-xylene content, as shown in Figure 2. Compared with the decane-rich systems, the increase in interlayer spacing is rather small whereas the  $a_s$  greatly increases. However, the  $a_s$  becomes almost constant in the L<sub>α</sub> phase. Since the  $a_s$  is also almost the same at the H<sub>1</sub>–L<sub>α</sub> transition point, the half thickness of the bilayer is half the radius of the cylinder micelle in the H<sub>1</sub> phase. The half thickness of the hydrophobic part in the L<sub>α</sub> phase is shorter than the surfactant hydrocarbon chain length in its extended form. It means that a considerable amount of oil is solubilized in the surfactant palisade layer because there is no pure oil layer in the L<sub>α</sub> phase. Since *m*-xylene is highly soluble in the surfactant palisade layer, it increases the volume of the hydrophobic part of the surfactant layer. It causes an increase in  $a_s$ . Since the adjacent EO chains are separated at large  $a_s$ , the reduction in repulsion would take place if the shape of the aggregates is unchanged. To balance the attraction and repulsion forces at a large  $a_s$ , the repulsion of the EO chain should be increased by changing the micellar shape. In fact, the EO chains



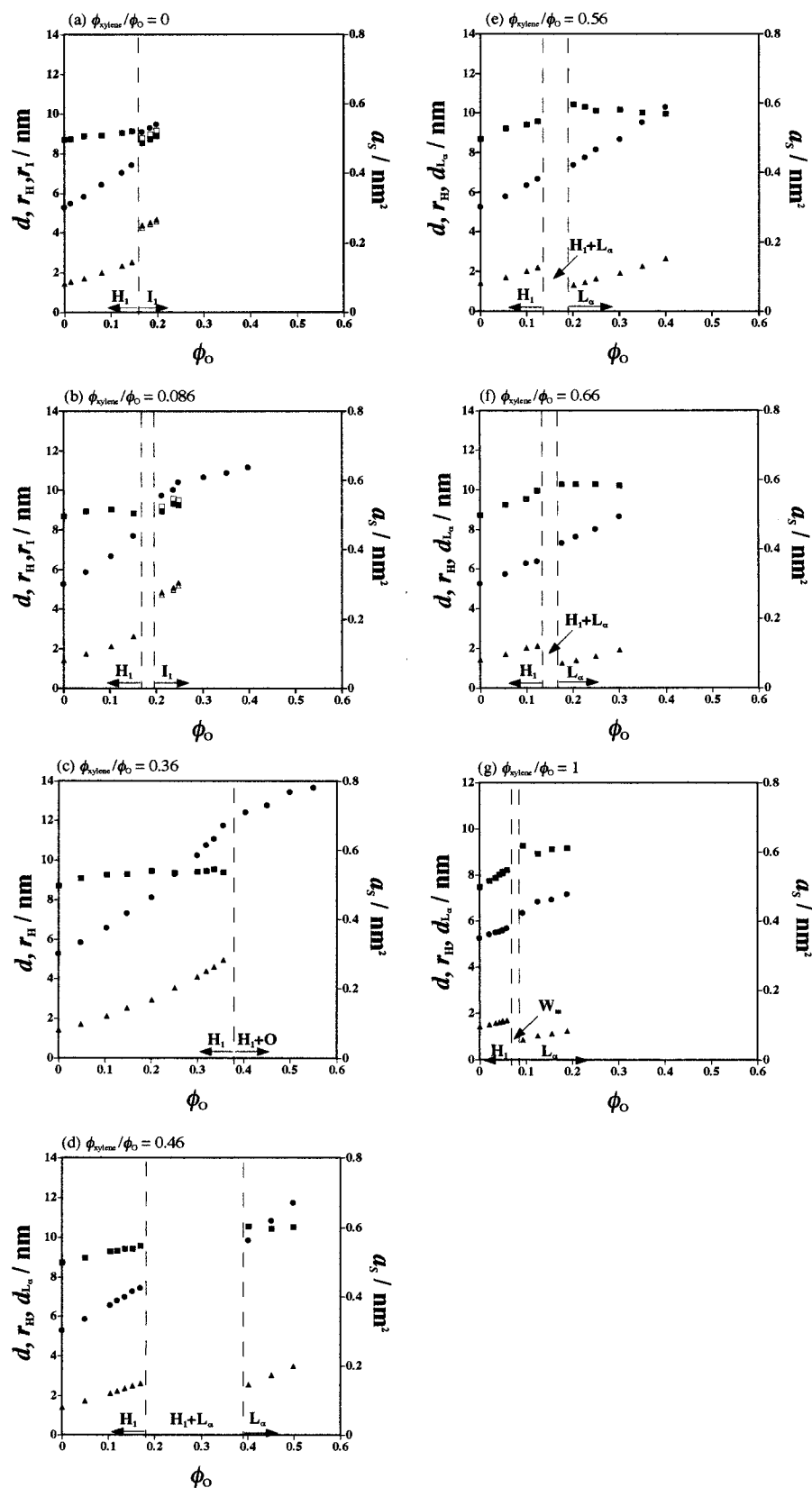


**Figure 4.** Change in  $r_H$ ,  $d_{L\alpha}$ , or  $r_L$  ( $\blacktriangle$ ) and effective cross sectional area  $a_S$  ( $\blacksquare$ ) at a fixed mixing fraction of *m*-xylene in the mixed oil. The measured interlayer spacing is also indicated by  $\bullet$ . The  $\phi_{xylenes}/\phi_O$  ratios are (a) 0, (b) 0.086, (c) 0.27, (d) 0.46, (e) 0.56, (f) 0.66, and (g) 1.0, respectively. Open and filled symbols for the  $I_1$  phase are the values for fcc and bcc, respectively.

approach each other in the  $L_\alpha$  phase, compared with the  $H_1$  phase.<sup>21</sup> This is the reason the  $H_1-L_\alpha$  transition takes place when *m*-xylene is solubilized.

**Mechanism of Phase Transition.** As described in the former sections, there is no drastic change in  $a_S$  at the transition of

$H_1-L_\alpha$  and  $H_1-I_1$ . Since it is considered that the attraction force due to the interfacial tension does not change greatly by the solubilization, the phase transition can be mainly attributed to the change in repulsion of the EO chains. When oil is solubilized in the rod micelles, the radius of the cylinder is increased. If

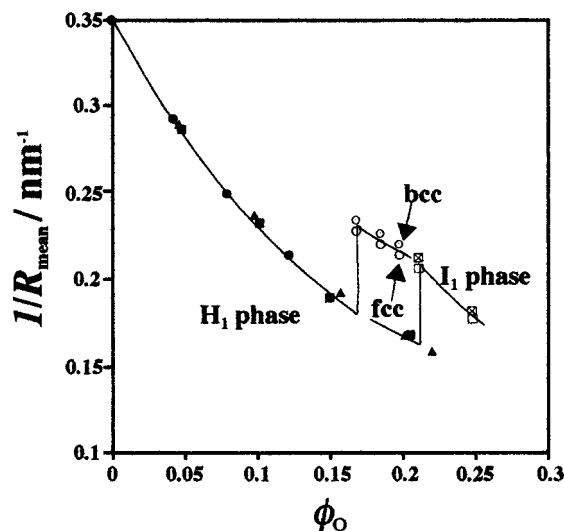


**Figure 5.** Change in the mean curvature of a cylindrical micelle [ $1/(2r_H)$ ] in the  $H_1$  phase or spherical micelle ( $1/r_H$ ) as a function of the oil content.  $\phi_{\text{xylene}}/\phi_O$  is fixed at 0 (●), 0.086 (■), 0.17 (▲).

the  $a_S$  remains constant, the hydrophilic moieties or EO chains are compressed because the cross sectional area occupied by one EO chain has to be shrunk, as is schematically shown in Figure 6a. In other words, the EO chain would be elongated if the cylinder radius increases because the distance between the adjacent EO chains becomes small because of the decrease in angle for  $a_S$  from the center of the micelle. It causes an increase in repulsion. On the other hand, if the  $a_S$  is largely increased, the cross sectional area per EO chain is laterally expanded. Since the EO chains are separated, the repulsion would decrease.

We consider the optimum sectional area per surfactant at the interface of the lipophilic part,  $a_{S,\text{opt}}$ , at which the average cross sectional area,  $\bar{a}_{EO}$ , of the EO chain is neither compressed nor expanded while oil is solubilized. We assumed that the attraction force due to the interfacial tension of the hydrophobic part is unchanged even if oil is solubilized in the aggregate. In the absence of oil, the effective cross sectional area,  $a_{S,0}$ , and the length of the EO chain of surfactant,  $r_{H,0}$ , are calculated by eqs

6 and 7 using the condition  $\phi_O = 0$ . According to the packing model, we calculate the EO chain length,  $r_{EO}$ , in the absence of oil by

$$r_{EO} = \alpha \left( \sqrt{\frac{\phi_S}{\phi_L}} - 1 \right) r_{H,0} \quad (11)$$

where  $\phi_S$  is the volume fraction of surfactant and  $r_{H,0}$  is the radius of the lipophilic cylinder.  $\alpha > 1$  is a correction factor to account for the hydration of the EO chain. When oil is solubilized in the cylinder micelles in the  $H_1$  phase, the radius of the lipophilic part is extended from  $r_{H,0}$  to  $r_H$  as shown in Figure 6b. It is considered that  $\bar{a}_{EO}$  is neither compressed nor expanded if  $r_{EO}$  remains constant as shown in Figure 6b. Then the balance between the repulsion and the attraction forces is unchanged, and the cylinder micelle remains stable.

Since the EO chain is hydrated by water, the real EO chain length would be longer than the present  $r_{EO}$  because the volume of the hydrophilic part is the sum of the EO chain and hydrated water. If it is assumed that the hydrated water is neglected and the space is filled by only the EO chain up to  $r_{EO}$ , then,  $\alpha = 1$ .

Since eq 7 holds for both actual  $a_S$  and  $a_{S,\text{opt}}$ , the following relation is valid.

$$\frac{a_S}{a_{S,\text{opt}}} = \frac{r_{H,\text{opt}}}{r_H} \quad (12)$$

where  $r_{H,\text{opt}}$  is the radius of lipophilic cylinder in which the effective cross sectional area is  $a_{S,\text{opt}}$ . Since

$$r_{H,\text{opt}}^2 / (r_{H,\text{opt}} + r_{EO})^2 = (\phi_L + \phi_O) / (\phi_S + \phi_O)$$

we obtain

$$\frac{a_S}{a_{S,\text{opt}}} = \frac{r_{EO}}{r_H} \left( \sqrt{\frac{\phi_S + \phi_O}{\phi_L + \phi_O}} - 1 \right)^{-1} \quad (13)$$

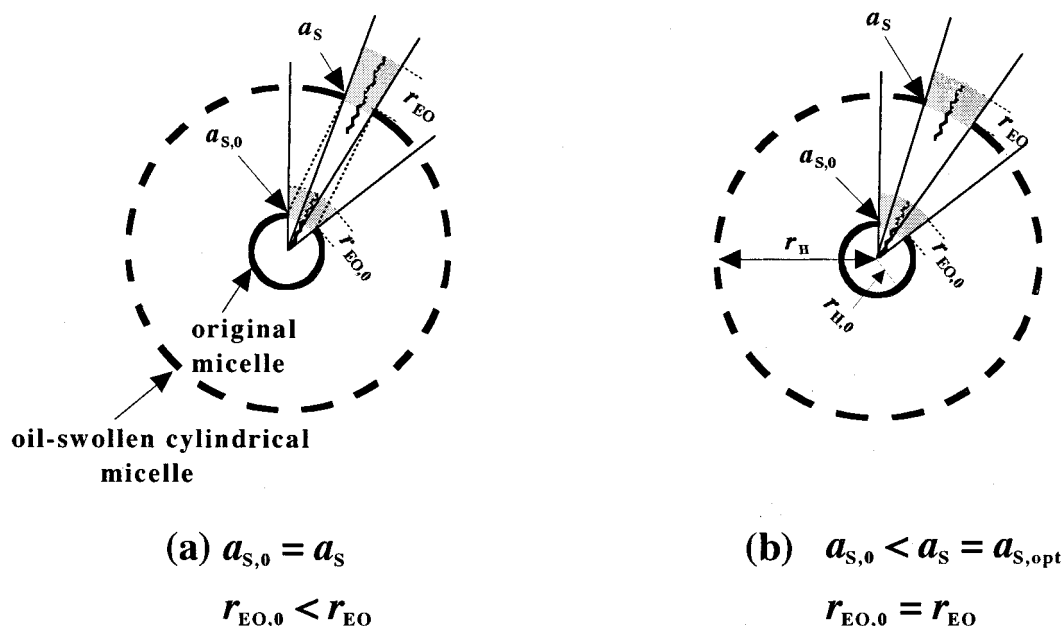


**Figure 6.** Schematic representation of the section of cylinder micelle in the  $H_1$  phase. The small circle is the section of the micelle in the absence of oil, whereas the large one is that of oil-swollen micelle. (a) If the  $a_S$  is constant while oil is swollen in the aggregate, the hydrophilic moiety is laterally compressed. (b) If the length of hydrophilic part,  $r_{EO}$ , is constant and equal to  $r_{EO,0}$ , the EO chain is neither compressed nor expanded.

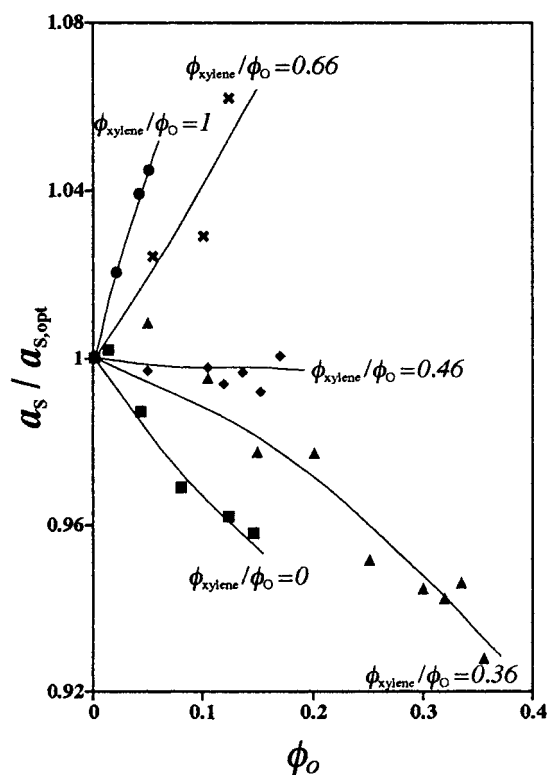


**Figure 7.**  $a_s/a_{s,opt}$  in the  $H_1$  phase as a function of  $\phi_O$ .  $a_s/a_{s,opt} < 1$  indicates that the repulsion of the surfactant EO chains increases with increasing oil content, whereas  $a_s/a_{s,opt} > 1$  means that the attraction of lipophilic moieties increases.  $a_s$  is the effective cross sectional area at the interface in the  $H_1$  phase in each oil system.  $a_{s,opt}$  is the optimum  $a_s$  at which the hydrophilic moieties or EO chains are neither compressed nor expanded upon an increase in the solubilization of oil.

Combining eqs 6, 11, and 13, we obtain

$$\frac{a_s}{a_{s,opt}} = \alpha \sqrt{\frac{3\pi}{2}} \frac{r_{H_0}(\sqrt{\phi_S} - \sqrt{\phi_L})}{\sqrt{\phi_L}(\sqrt{\phi_S + \phi_O} - \sqrt{\phi_L + \phi_O})} \frac{1}{d} \quad (14)$$

Since we do not know  $\alpha$ , we calculate  $a_s/a_{s,opt}$  assuming  $\alpha = 1$ , and the results are shown in Figure 7.

Equation 14 shows how the EO chain is compressed or expanded when oil is solubilized. When  $a_s/a_{s,opt}$  is unity, the EO chain is neither compressed nor expanded while solubilization proceeds. It means that the repulsion is unchanged. In the decane system,  $a_s/a_{s,opt}$  decreases with increasing oil content. The repulsion of the EO chain is increased because of the decrease in distance between the EO chains. Hence, if oil is solubilized in the deep core of the aggregates and the radius of cylinder micelle increases, the repulsion increases. To keep the balance between both repulsion and attraction forces, the  $H_1$ – $I_1$  transition takes place in order to decrease the repulsion between the EO chains. When the micellar shape is changed from rod to sphere, the EO chains can separate even at the same  $a_s$ .

In contrast, in the *m*-xylene system,  $a_s/a_{s,opt}$  increases upon addition of oil. It means that the repulsion is decreased when the cylinder micelle is swollen by oil. Then the attraction force becomes larger than the repulsion. If the cylinder micelle changes to the layer structure, the distance between the EO chains becomes short and the repulsion would increase at the same  $a_s$ . It is considered that the largest solubilization can be attained at  $a_s/a_{s,opt} = 1$ . In Figure 7,  $a_s/a_{s,opt} = 1$  holds at  $\phi_{xylene}/\phi_O = 0.46$ . However, the  $H_1$  phase can solubilize the largest

amount of oil at  $\phi_{xylene}/\phi_O$  below 0.4 as is shown in Figure 2. In our calculation, we assume that the hydration of the EO chain was neglected and that  $\alpha = 1$ . Since  $\alpha$  should be larger than 1, the calculated  $a_s/a_{s,opt}$  in Figure 7 is smaller than the real value. This may be the reason for the error. Furthermore, it is also assumed that the attraction due to interfacial tension is constant even if solubilization progresses. This may also be the reason for the deviation.

## Conclusions

The effect of mixing oils (*m*-xylene + decane) on the phase behavior in a water/ $C_{12}EO_7$ /oil system is similar to that of temperature. When decane is solubilized in the  $H_1$  phase, the rod–sphere transition takes place, whereas the opposite phase transition from the  $H_1$  to the  $L_\alpha$  phase occurs in the *m*-xylene-rich systems. Because of the opposite phenomena, the surfactant layer curvature abruptly changes from positive to negative in a narrow range of mixing fractions of *m*-xylene in the mixed oil or temperatures in the presence of a sufficient amount of oil. The SAXS results show that the effective cross sectional area per surfactant molecule at the water–hydrocarbon chain interface,  $a_s$ , is not largely increased in the decane system whereas the  $a_s$  considerably increases in the *m*-xylene system, since the  $a_s$  values are nearly constant at both  $H_1$ – $I_1$ , and  $H_1$ – $L_\alpha$  transitions. Thus, the phase transitions are attributed to the change in repulsion of the EO chains. The simple geometrical relation shows that the repulsion between the EO chains increases with increasing decane content. For the relaxation of the compressed EO chain, the  $H_1$ – $I_1$  transition takes place. On the other hand, the repulsion decreases in the *m*-xylene system because the  $a_s$  is larger than the optimum  $a_s$  because of the penetration of the oil in the surfactant palisade layer.

## References and Notes

- (1) Shinoda, K.; Friberg, S. E. *Emulsions and Solubilization*; John Wiley: New York, 1986; Chapter 3.
- (2) Hoffman, H.; Ulbricht, W. *J. Colloid Interface Sci.* **1989**, *129*, 388.
- (3) Kunieda, H.; Ozawa, K.; Huang, K.-L. *J. Phys. Chem. B* **1998**, *102*, 831.
- (4) Holmqvist, P.; Alexandridis, P.; Lindman, B. *J. Phys. Chem. B* **1998**, *102*, 1149.
- (5) Chen, S. J.; Evans, D. F.; Ninham, B. W.; Mitchell, D. J.; Blum, F. D.; Pickup, S. *J. Phys. Chem. B* **1986**, *90*, 842.
- (6) Warr, G. G.; Sen, R.; Evans, D. F.; Trend, J. E. *J. Phys. Chem. B* **1988**, *92*, 774.
- (7) Eastoe, J.; Hetherington, K. J.; Sharpe, D.; Dong, J.; Heenan, R. K.; Steytler, D. *Langmuir* **1996**, *12*, 3876.
- (8) Kunieda, H.; Shigeta, K.; Ozawa, K.; Suzuki, M. *J. Phys. Chem. B* **1997**, *101*, 7952.
- (9) Kunieda, H.; Friberg, S. E. *Bull. Chem. Soc. Jpn.* **1981**, *54*, 1010.
- (10) Kunieda, H.; Shinoda, K. *J. Colloid Interface Sci.* **1985**, *107*, 107.
- (11) Tanford, C. *J. Phys. Chem. B* **1972**, *76*, 3020.
- (12) Huang, K.-L.; Shigeta, K.; Kunieda, H. *Prog. Colloid Polym. Sci.* **1998**, *110*, 171.
- (13) Ekall, P.; Mandell, P.; Fontell, K. *J. Colloid Interface Sci.* **1970**, *33*, 215.
- (14) Aramaki, K.; Kunieda, H. *Colloid Polym. Sci.* **1999**, *34*, 277.
- (15) Fontell, K. *Colloid Polym. Sci.* **1990**, *268*, 264.
- (16) Sakya, P.; Seddon, J. M.; Templer, R. H.; Mirkin, R. J.; Tiddy, G. J. T. *Langmuir* **1997**, *13*, 3706.
- (17) Strey, R.; Schomäcker, R.; Roux, D.; Nallet, F.; Olsson, U. *J. Chem. Soc., Faraday Trans.* **1990**, *86*, 2253.
- (18) Griffin, W. C. *J. Soc. Cosmet. Chem.* **1954**, *5*, 249.
- (19) Israelachvili, J. N.; Mitchell, D. J.; Ninham, B. W. *J. Chem. Soc., Faraday Trans. 2* **1976**, *72*, 1525.
- (20) Hyde, S.; Anderson, S.; Larsson, K.; Blum, Z.; Lauth, T.; Lindin, S.; Ninham, B. W. *The Language of Shape*; Elsevier: Amsterdam 1997; Chapters 3 and 4.
- (21) Kunieda, H.; Umizu, G.; Yamaguchi, Y.; Suzuki, M. *J. Jpn. Oil Chem. Soc.* **1998**, *47*, 879.